Polymer 50 (2009) 5211–5219

Contents lists available at ScienceDirect

Polymer

journal homepage: www.elsevier.com/locate/polymer

New amphiphilic fluorescent CBABC-type pentablock copolymers containing pyrene group by two-step atom transfer radical polymerization (ATRP) and its self-assembled aggregation

Wen-Hsiang Chen [a], Der-Jang Liaw [a,*], Kun-Li Wang [b], Kueir-Rarn Lee [c], Juin-Yih Lai [c]

[a] Department of Chemical Engineering, National Taiwan University of Science and Technology, 10607, Taipei, Taiwan
[b] Department of Chemical Engineering and Biotechnology, National Taipei University of Technology, 10608, Taipei, Taiwan
[c] R&D Center for Membr. Technol., Department of Chemical Engineering, Chung Yuan University, 32023, Chung-Li, Taiwan

ARTICLE INFO

Article history:
Received 22 April 2009
Received in revised form
4 August 2009
Accepted 14 August 2009
Available online 6 September 2009

Keywords:
ATRP
Amphiphilic
Pentablock

ABSTRACT

A series of novel amphiphilic fluorescent CBABC-type pentablock copolymers (**Py–PMMA–PEG4600–PMMA–Py**) were prepared from BAB-type amphiphilic triblock copolymer (**PMMA–PEG4600–PMMA**) as macroinitiator with various contents of 1-(methacryloyloxyethylamino-carboxylmethyl) pyrene (**PyMOI**) by atom transfer radical polymerization (ATRP) in toluene using CuBr/2,2-bipyridine as catalyst system. Triblock copolymer (**PMMA–PEG4600–PMMA**) was prepared by ATRP and obtained from **Br–PEG4600–Br** as macroinitiator with methyl methacrylate in tetrahydrofuran using the same catalyst. The molecular weights of pentablock copolymers which were reinitiated by **PMMA–PEG4600–PMMA** macroinitiator were calculated from ^{1}H NMR spectra up to 42,400 gmol^{-1}. The polydispersity of pentablock copolymers obtained from GPC analysis was narrow between 1.10 and 1.38. The crystallinity of triblock copolymer (**PMMA–PEG4600–PMMA**) was decreased slightly with incorporating PMMA segment. Introducing the bulky pyrene substituent into pentablock copolymer, the melting temperature was not observed and all pentablock copolymers showed amorphous patterns in wide-angle X-ray scattering (WAXS) due to decrease in the degree of crystallinity of polymer chain because of disturbing regular packing. The temperatures at 10% weight loss (Td_{10}), examined by TG analysis, showed values ranging from 265 to 323 °C in nitrogen and 264 to 313 °C in air. Fluorescence spectra of **Py–PMMA–PEG4600–PMMA–Py** exhibited stronger excimer emission at *ca.* 480 nm due to the aggregations of pyrene group formed *via* interaction of the hydrophobic chains. The more content of **PyMOI** segment in pentablock copolymers can obtain the higher emission intensity *ca.* 480 nm. When there were higher **PyMOI** contents (84.9 wt% **PyMOI**) in pentablock copolymers, they formed larger aggregates (210 nm) in SEM micrographs. On the other hand, while increasing the concentration of the polymer solution in THF, the morphology was changed from spherical (0.1 mg/mL) to chainlike (1.0 mg/mL) aggregates.

1. Introduction

Block copolymers are important materials, which can be synthesized with tailor-made properties using different available synthetic methodology [1]. Well-defined block copolymers are generally synthesized using ionic living polymerization technique [2]. Recently, controlled/living radical polymerizations (CRP) are widely used to synthesize a range of new polymeric materials. Controlled/living radical polymerization (CRP) has emerged in the last decade with an explosion of academic and industrial research, leading to one of the most active fields of research in polymer chemistry [3–17]. This technique offers many advantages over conventional living ionic polymerization [2].

There have been only few publications on linear CBABC-type pentablock copolymers using different polymerization techniques [18–21]. This type of multicompartment aggregates that are able to mimic basic properties of natural systems such as serum albumins is significant in nanotechnology [20,22–24]. Its applications in medicine, pharmacy, biotechnology, and so forth seem to be possible, but the preparation and control of stable multicompartment micellar systems are still at the very beginning. To our knowledge, there are some reports for block copolymers by two-step polymerization [25–29]. However, there are only few reports for CBABC-type pentablock copolymers by two-step atom transfer radical polymerization [30,31].

* Corresponding author. Tel.: +886 2 27376638/35050; fax: +886 2 23781441/7376644.
E-mail addresses: liawdj@mail.ntust.edu.tw, liaw6565@yahoo.com.tw (D.-J. Liaw).

0032-3861/$ – see front matter © 2009 Elsevier Ltd. All rights reserved.
doi:10.1016/j.polymer.2009.08.042

Methyl methacrylate (MMA) is a well-known living monomer for copper-based ATRP systems [3]. Some literatures [21,32–35] stated that multiblock copolymers were synthesized by using PMMA as bridge block which connected initiator and the other monomers in ATRP. For example, Eastwood et al. [34] reported that multiblock copolymers of methyl methacrylate and styrene were synthesized by ATRP regardless of monomer sequence. That means the polymer chain end of triblock copolymer is still carrying out in controlled/"living" free radical polymerization. On the other hand, fluorescent labeling technique is a quite useful way to study association properties of polymeric materials [36–41]. Pyrene is often attached to polymers as a fluorescent probe serving as an active association site of amphiphilic copolymers in solution [36,37]. In addition, the monomer containing pyrene group can apply to membrane and biochemistry field [38].

In this paper, the synthesis of novel amphiphilic fluorescent CBABC-type pentablock copolymers based on PEG (block A) [42] as hydrophilic segment, amorphous PMMA (block B) and **PyMOI** (block C) [43] as hydrophobic segments by two-step ATRP will be concentrated. The aim of the research is to investigate the compatibility among three different components, the crystallization behavior of PEG in this pentablock system and its self-assembled aggregation. The synthesis and characterization of these novel amphiphilic fluorescent pentablock copolymers such as molecular weight, thermal and optical properties as well as the size and morphologies of aggregates are also investigated and discussed.

2. Experimental

2.1. Materials

Methyl methacrylate (MMA) was washed multiple times with 5% sodium hydroxide solution and 20% sodium chloride to remove the stabilizer. After drying over magnesium sulfate, the methyl methacrylate was purified by vacuum distillation. Poly(ethylene glycol) 4600 (PEG 4600, $\overline{M}_n = 4600$) was purchased from Aldrich and was dried by azeotropic distillation with toluene prior to use. Triethylamine (TEA) was dried over magnesium sulfate, filtered, distilled, and stored over 4 Å molecular sieves. Copper (I) halides were obtained from Aldrich and purified according to the method reported in preceding studies [44]. The chemical reagents, 2-bromoisobutyryl bromide, 1-pyrenemethanol, 2-methacryloyl oxyethyl isocyanate (MOI), dibutyltin dilaurate (DBTDL) and 2,2′-bipyridine (bipy) were purchased from Aldrich and used as received without purification. Solvents were dried by standard process.

2.2. Synthesis of 1-(methacryloyloxyethylaminocarboxyl-methyl)pyrene (*PyMOI*) (Scheme 1)

The **PyMOI** was synthesized as outlined in Scheme 1. A 150 mL round-bottom flask was charged with a mixture of 1-pyrenemethanol (4.3 mmol), DBTDL (10 drops) and anhydrous tetrahydrofuran (30 mL) and maintained in an ice bath under dry nitrogen atmosphere. The active reagent, 2-methacryloyl oxyethyl isocyanate (MOI) (6.5 mmol) was dissolved in anhydrous tetrahydrofuran (20 mL), and then added to the above reaction mixture from a dropping funnel over a period of 1 h under dry nitrogen at 0 °C; subsequently the temperature was allowed to rise to room temperature. The reaction was continued under stirring for 24 h. After completion of reaction, the solution was concentrated, then purified by column chromatography (silica, eluent: CH_2Cl_2) to yield pure **PyMOI** as a light yellow powder. Yield: 94.5%, m.p. 98 °C (by DSC at a scan rate of 10 °C min^{-1}). The FT-IR spectrum of **PyMOI** (KBr pellet) exhibited absorptions at 3299 (N–H stretching), 1712 (ester C=O), 1689 (urethane C=O), 1638 (C=C) and 1549 cm^{-1} (N–H bending). ^{1}H NMR (500 MHz, $CDCl_3$): δ(ppm) 8.13–7.84 (9H, H_1), 6.00 and 5.43 (2H, H_6), 5.69 (2H, H_2), 5.23 (1H, H_3), 4.17 (2H, H_5), 3.45 (2H, H_4), 1.83(3H, H_7); ^{13}C NMR (125 MHz, $CDCl_3$): δ(ppm) = 167.09 (C_9), 156.37 (C_8), 135.75 (C_{10}), 131.42–122.68 (C_1), 125.81 (C_6), 65.11 (C_2), 63.47 (C_5), 40.09 (C_4), 18.07 (C_7).

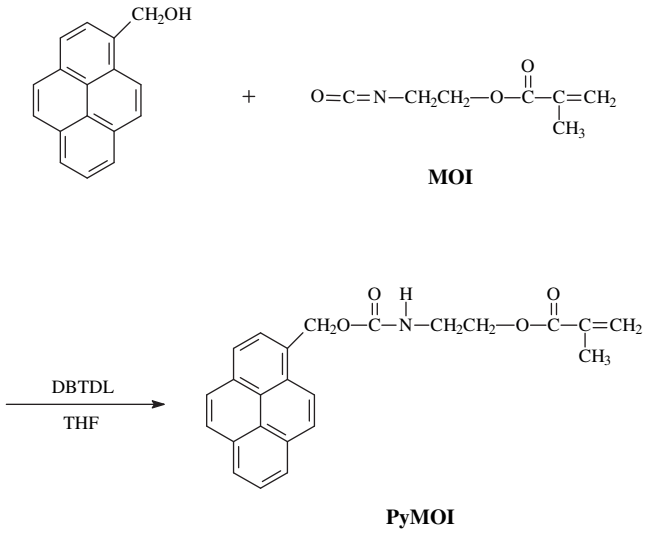

Scheme 1. Synthesis route of 1-(methacryloyloxyethylaminocarboxyl methyl)pyrene (**PyMOI**).

Anal. Calcd for $C_{24}H_{21}O_4N$: C, 74.40%; H, 5.46%; N, 3.62%; Found: C, 74.13%; H, 5.61%; N, 3.55%

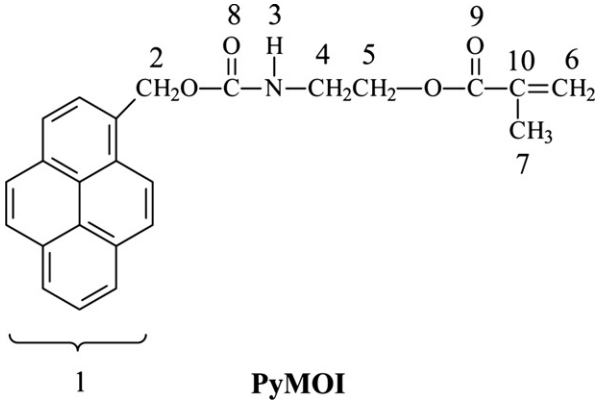

2.3. Synthesis of PEG macroinitiator (*Br–PEG4600–Br*) (Scheme 2)

The macroinitiator PEG4600 (**Br–PEG4600–Br**) was synthesized as outlined in Scheme 2. A mixture of PEG4600 (10 g, 2.17 mmol) in dry methylene chloride (50 mL) and triethylamine (TEA) (1.21 mL, 8.69 mmol) was charged into a round-bottom flask (150 mL) and maintained in an ice bath. The active reagent, 2-bromoisobutyryl bromide (1.61 mL, 13.04 mmol) was dissolved in methylene chloride (30 mL), and then added to the above reaction mixture from a dropping funnel over a period of 1 h under dry nitrogen; subsequently the temperature was allowed to rise to room temperature. The reaction was continued under stirring for 24 h. After completion of reaction, the solution was filtered, then was poured into water to wash multiple times and extracted with methylene chloride. The organic extract was washed successively with 1 M HCl, 1 M NaOH and 1% Na_2CO_3 solution and extracted using methylene chloride. The collected organic layer was dried over $MgSO_4$

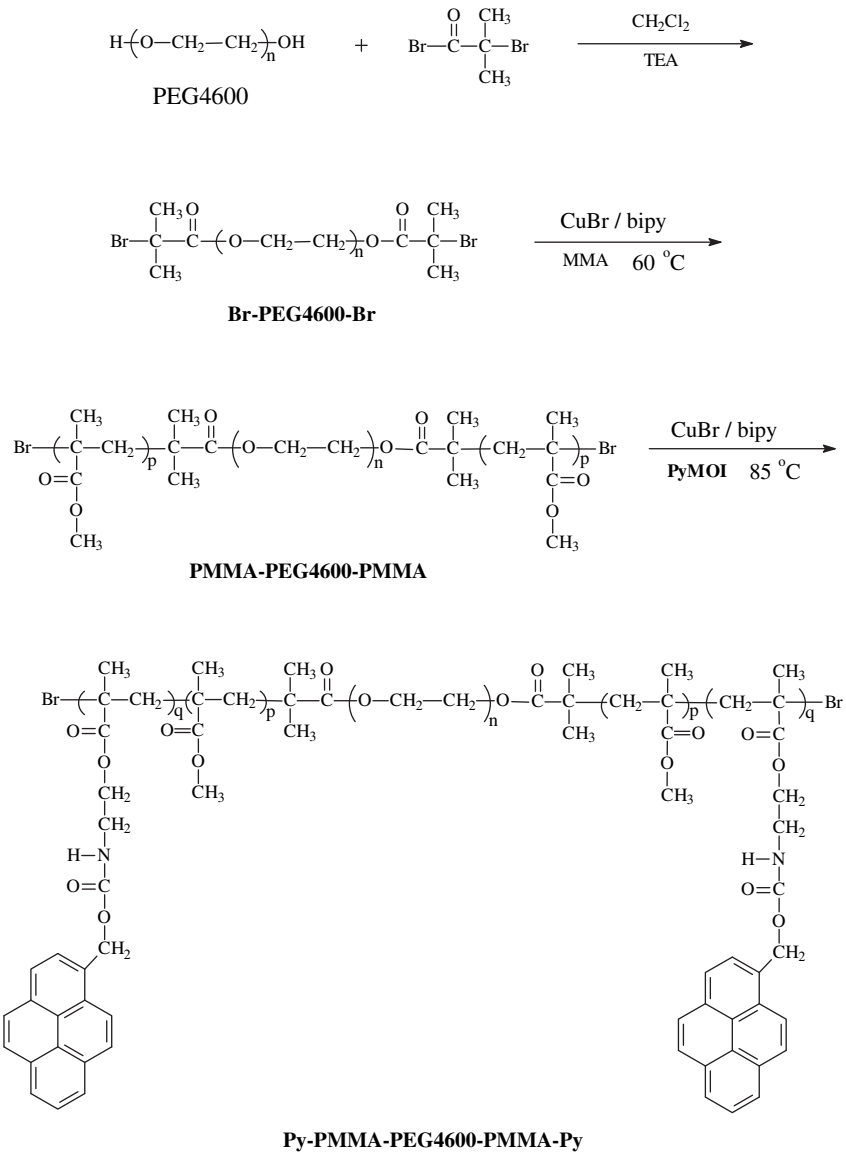

Scheme 2. Synthesis route of **Br–PEG4600–Br**, **PMMA–PEG4600–PMMA** triblock copolymer and **Py–PMMA–PEG4600–PMMA–Py** pentablock copolymer.

overnight, and the solvent was removed under reduced pressure. The concentrated solution was precipitated from ether, dissolved in CH_2Cl_2 and reprecipitated from ether multiple times, after which the macroinitiator was collected and dried under vacuum for one day at room temperature. After drying, the pure macroinitiator **Br–PEG4600–Br** was obtained. Yield: 57%. m.p. 53.2 °C (by DSC at a scan rate of 10 °C min^{-1}). The FT-IR spectrum of **Br–PEG4600–Br** exhibited absorptions at 1740 cm^{-1} (C=O) and 1112 cm^{-1} (C–O–C). ^1H NMR (500 MHz, $CDCl_3$) of **Br–PEG4600–Br**: δ(ppm) 4.25 (4H, H_2), 3.71–3.43 (440H, H_1), 1.87 (12H, H_3); ^{13}C NMR (125 MHz, $CDCl_3$): δ(ppm) = 171.36 (C_4), 70.31 (C_1), 64.90 (C_2), 55.52 (C_5), 30.54 (C_3).

*2.4. Synthesis of triblock copolymer with PMMA segment derived from macroinitiator (**Br–PEG4600–Br**) via ATRP (**PMMA–PEG4600–PMMA**)*

The synthetic route of **PMMA–PEG4600–PMMA** is outlined in Scheme 2. To an ampoule, CuBr (0.0268 g, 1.87×10^{-4} mol), 2,2′-bipyridine (0.0584 g, 3.74×10^{-4} mol), **Br–PEG4600–Br** [$\overline{M}_n$ = 5200 g/mol (obtained from ^1H NMR)] (0.9711 g, 1.87×10^{-4} mol) and MMA (0.1872 g, 18.7×10^{-4} mol) were added in 5 mL anhydrous THF. The heterogeneous mixture was frozen and placed under vacuum and then degassed *via* a freeze-pump-thaw cycle thrice. After degassing three times, the ampoule was stirred at

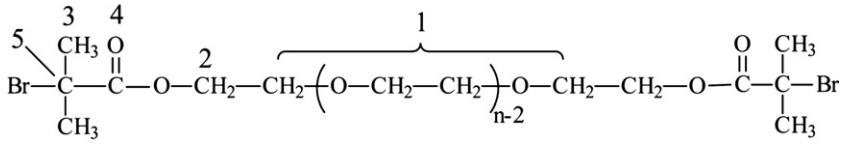

60 °C for 20 h. After completion of the reaction and the reaction mixture cool down to room temperature, THF was added to the ampoule and then was passed through a silica column (SiO_2) to remove the copper complex. The resulting colorless polymer, **PMMA–PEG4600–PMMA**, was precipitated from ether, dissolved in CH_2Cl_2 and reprecipitated from ether multiple times, after which the polymer was collected and dried under vacuum for one day at room temperature. m.p. 48.7 °C (by DSC at a scan rate of 10 °C min^{-1}). The FT-IR spectrum of **PMMA–PEG4600–PMMA** exhibited absorptions at 1727 cm^{-1} (C═O) and 1103 cm^{-1} (C–O–C). ^{1}H NMR ($CDCl_3$): δ (ppm) 4.33 (4H, H_6hHhhh), 3.82–3.46 (476H, H_1 and H_5), 2.01–1.81(24H, H_3), 1.94(12H, H_2), 1.17–0.84 (36H, H_4).

2.5. Synthesis of pentablock copolymer with pyrene segment derived from macroinitiator (*PMMA–PEG4600–PMMA*) via ATRP (*Py–PMMA–PEG4600–PMMA–Py*)

The synthetic route of **Py–PMMA–PEG4600–PMMA–Py** is outlined in Scheme 2. In a typical run, to an ampoule, CuBr (1.12 mg, 7.81×10^{-3} mmol), 2,2′-bipyridine (2.44 mg, 15.6×10^{-3} mmol), **PMMA–PEG4600–PMMA** [$\overline{M}_n$ = 6400 (obtained from ^{1}H NMR)] (0.05 g, 7.81×10^{-3} mmol) and **PyMOI** (0.1513 g, 3.9×10^{-4} mol) were added in 2 mL anhydrous toluene. The heterogeneous mixture was frozen and placed under vacuum and then degassed *via* a freeze-pump-thaw cycle thrice. After degassing three times, the ampoule was stirred at 85 °C for 20 h. After completion of the reaction and the reaction mixture cool down to room temperature, THF was added to the ampoule and then was passed through a silica column (SiO_2) to remove the copper complex. The resulting colorless polymer, **Py–PMMA–PEG4600–PMMA–Py**, was precipitated from methanol, dissolved in CH_2Cl_2 and reprecipitated from methanol multiple times, after which the polymer was collected and dried under vacuum for 1 day at room temperature. The FT-IR spectrum of **Py–PMMA–PEG4600–PMMA–Py** exhibited absorptions at 3402 cm^{-1} (N–H), 1721 cm^{-1} (C═O) and 1134 cm^{-1} (C–O–C). ^{1}H NMR ($CDCl_3$): δ (ppm) 7.70–7.47(423H, H_{11}), 5.58–5.39(141H, H_9 and H_{10}), 3.95–3.13(664H, H_1, H_5 and H_8), 1.88–1.59(130H, H_2, H_3 and H_6), 1.02–0.84(177H, H_4 and H_7).

2.6. Measurements

FT-IR spectra were recorded in the range 4000–400 cm^{-1} on a Bio-Rad FTS-3500 spectrometer. Elemental analyses were performed on Perkin–Elmer 2400 C, H, and N analyzer. The ^{1}H and ^{13}C NMR spectra were recorded on a Bruker DRX-500 instrument operating at 500 MHz for proton and 125 MHz for carbon. The melting temperature (T_m), glass transition temperature (T_g) and the melting enthalpy (δH_m) were measured on a Du Pont 9000 differential scanning calorimeter at a heating rate of 10 °C min^{-1} from −50 to 150 °C under a steady flow of nitrogen (30 cm^3 min^{-1}). The data were recorded on second run heating. The recorded temperatures were calibrated using Indium as standard. Wide angle X-ray scattering (WAXS) patterns were recorded at room temperature with powder on an X-ray scattering (Osmic, USA; PSAXS-USH-WAXS-002) using 30 W low power X-ray source/optic combination that provides Cu K alpha radiation (45 kV, 0.67 mA). Thermogravimetric (TG) data were obtained on a Du Pont Q 500 TGA at a heating rate of 10 °C min^{-1} from 30 to 600 °C under nitrogen flowing conditions (60 cm^3 min^{-1}). Weight-average ($\overline{M}_w$) and number-average ($\overline{M}_n$) molecular weight were determined by gel permeation chromatography (GPC). Five Waters (Ultrastyragel) columns 300 × 7.7 mm (guard, 500, 10^3, 10^4, 10^5 Å in a series) were used for GPC analysis with tetrahydrofuran (THF) (1 mL min^{-1}) as an eluent. The eluents were monitored with a refractive index detector (RI 2000). Polystyrene was used as a standard. The fluorescence spectra were recorded by a Shimadzu RF-5031 spectrophotometer. The polymer solutions were mixed at predetermined ratios. All the fluorescence measurements were performed in THF at constant concentration (1.85×10^{-4} mg/mL) and room temperature by excitation at 330 nm wavelength. Morphology observations were performed with a Hitachi S-2400 scanning electron microscope at an accelerating voltage of 20 kV. The specimens for SEM observations were prepared by depositing a drop of the aggregate solutions having polymer concentration of 0.1 mg/mL or 1 mg/mL in THF onto a glass slide and then they were gold sputtered (Hitachi E101 Ion sputter) under vacuum.

3. Results and discussion

3.1. Synthesis and characterization of *PyMOI*

PyMOI was synthesized by the reaction of 1-pyrenemethanol with MOI in THF, as shown in Scheme 1.

After purification by column chromatography (silica gel, eluent: CH_2Cl_2) to yield pure **PyMOI** (Yield = 95%), the structure of the **PyMOI** was confirmed by elemental analysis, FT-IR and NMR spectroscopies. The FT-IR spectrum of **PyMOI** showed absorption bands at 3299 (N–H stretching), 1712 (ester C═O), 1689 (urethane C═O), 1638 (C═C) and 1549 (N–H bending), confirmed the presence of vinyl and urethane groups in the structure. The results of ^{1}H NMR and ^{13}C NMR spectrum of **PyMOI** are described in experimental section. The resonance signals at downfield regions (δ(ppm): 8.13–7.84) in the ^{1}H NMR spectrum are ascribed to the protons of pyrene group. The vinylic proton in ^{1}H NMR spectrum peaks appeared at 6.00 and 5.43 ppm. The area of integration for the protons is in accordance with the assignment. In ^{13}C NMR spectrum, the signals of vinylic carbons at 125.81 and 135.75 ppm, the signals of carbonyl group of urethane and ester group at 156.37 ppm and 167.09 ppm, respectively, and the signal of methyl carbon of methacryloyl group at 18.07 ppm were observed. The product, **PyMOI** was not observed the hydroxyl group of 1-pyrenemethanol in FT-IR and NMR spectra. These results clearly confirm that the monomer **PyMOI** prepared herein is consistent with the proposed structure. The results of the elemental analyses are also in good agreement with the calculated ones.

3.2. Synthesis and characterization of macroinitiator *Br–PEG4600–Br* and copolymers

In Scheme 2, the synthesis route of **Br–PEG4600–Br**, **PMMA–PEG4600–PMMA** and **Py–PMMA–PEG4600–PMMA–Py** is outlined.

The macroinitiator was synthesized by coupling poly(ethylene glycol) to 2-bromoisobutyryl bromide. Esterification of PEG4600 with 2-bromoisobutyryl bromide was carried out at 0 °C under dry nitrogen atmosphere according to the literature [45,46]. The structure of the macroinitiator was confirmed by FT-IR and NMR spectroscopes. The FT-IR spectrum of **Br–PEG4600–Br** showed absorption bands at 1740 (ester C═O stretching) and 1112 cm^{-1} (C–O–C stretching vibration), confirmed the presence of poly(ethylene glycol) and ester groups in the structure. The crystalline phase of PEG revealed the characteristic absorptions at 949 and 843 cm^{-1} [47]. The intensities of two peaks are associated with PEG segment and its crystallinity. The ^{1}H NMR spectrum and assignment of the signals for the macroinitiator **Br–PEG4600–Br** are depicted in Fig. 1(a).

In ^{1}H NMR spectrum, the hydroxyl group (–OH) disappears, and the new signals at 4.25 (peak 2) and 1.87 (peak 3) ppm appear for the **Br–PEG4600–Br** macroinitiator in $CDCl_3$ after esterification. To enable the hydroxyl groups to be completely substituted, the feed molar ratio of 2-bromoisobutyryl bromide to PEG was five times.

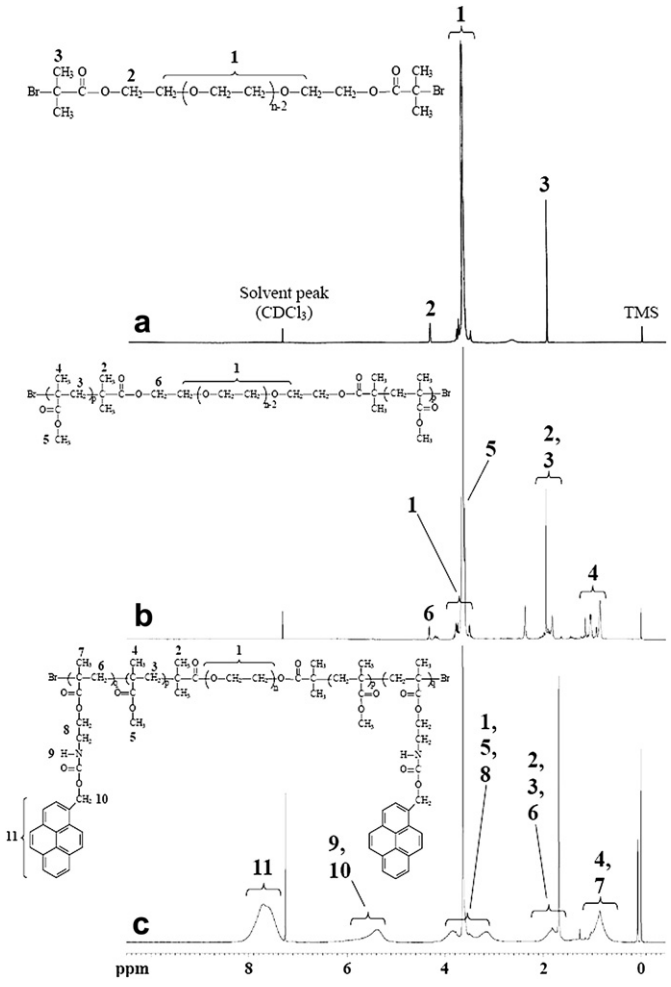

Fig. 1. The ^{1}H NMR spectrum (500 MHz) of (a) **Br–PEG4600–Br**, (b) **PMMA–PEG4600–PMMA**, (c) **Py–PMMA–PEG4600–PMMA–Py-1** in $CDCl_3$ at room temperature.

From the ^{1}H NMR spectra of PEG4600 and **Br–PEG4600–Br**, the integral ratio of peaks 2 and 3 is 1:3. These evidences suggest that the hydroxyl group is completely substituted and the macroinitiator is a difunctional initiator. By the integral ratio of peaks 3 and 1 of ^{1}H NMR in Fig. 1(a), absolute molecular weight of **Br–PEG4600–Br** was calculated to be 5.20×10^3 g/mol with 111 repeat units of PEG segment ($n = 111$ determined by ^{1}H NMR) in the PEG macroinitiator were obtained.

The preparation of well-defined amphiphilic triblock copolymers (**PMMA–PEG4600–PMMA**) *via* PEG-base initiator could be allowed by ATRP. The CuBr/bipy catalyst system was used in the

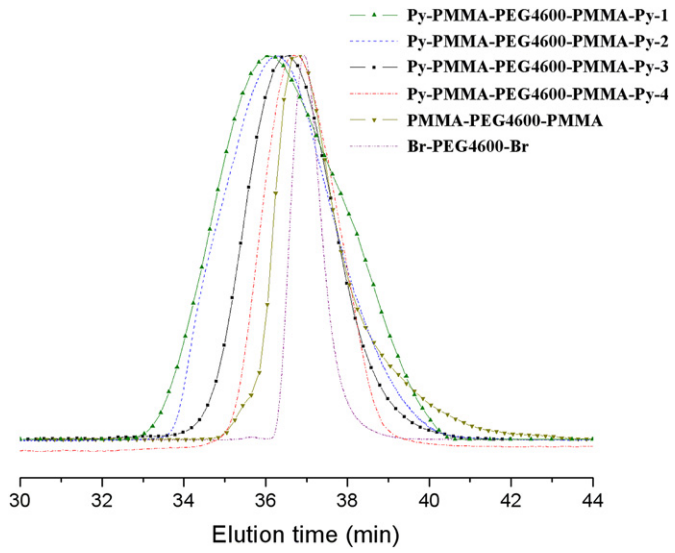

Fig. 2. The GPC traces of pentablock copolymers and their precursors.

polymerization of MMA by using **Br–PEG4600–Br** as an initiator. The reaction was carried out in THF at 60 °C and the molar ratio of MMA/**Br–PEG4600–Br**/CuBr/bipy was 10:1:1:2. The structure of the triblock copolymer was confirmed by FT-IR and NMR spectroscopies. The FT-IR spectrum of triblock copolymer, **PMMA–PEG4600–PMMA**, showed absorption bands at 1727 (ester C=O stretching for PMMA) and 1103 cm^{-1} (C–O–C stretching vibration), confirmed the presence of poly(ethylene glycol) and ester groups of PMMA segment in the structure. The crystalline phase of PEG also revealed the characteristic absorptions at 941 and 841 cm^{-1}. The ^{1}H NMR spectrum of triblock copolymer is presented in Fig. 1(b). The ^{1}H NMR spectrum of block copolymers which was obtained from macroinitiator (**Br–PEG4600–Br**) and MMA *via* ATRP exhibited signals at 3.60 ppm [–$CH_2C(CH_3)COOC\underline{H}_3$, peak 5 in Fig. 1(b)], 0.84–1.2 ppm due to proton of –$CH_2C(C\underline{H}_3)COOCH_3$. This observation confirmed the blocking of macroinitiator with MMA. From the weight fraction of PMMA in triblock copolymer (f_{MMA}) (Calculation detail was described in the Supplementary materials, Eq. S1) and $\overline{M}_n$ estimated by ^{1}H NMR of **Br–PEG4600–Br**, the absolute molecular weight of the corresponding **PMMA–PEG4600–PMMA** was calculated to be 6.40×10^3 g/mol with 12 repeat units of MMA segment ($2p = 12$, Scheme 2) in the triblock copolymer as shown in Table 1.

The pentablock copolymers, **Py–PMMA–PEG4600–PMMA–Py**, were subsequently prepared from **PyMOI**, **PMMA–PEG4600–PMMA** (6.40×10^3 g/mol from ^{1}H NMR) as initiator and CuBr/bipy as catalyst *via* ATRP. The reaction was carried out in toluene at 85 °C

Table 1
Yield, GPC and ^{1}H NMR data of the CBABC-type pentablock copolymers and their precursors.

Sample code	Yield[a] %	$\overline{M}_n \times 10^{-3}$[b]	PDI[c]	wt% PEO[d]	wt% PMMA[d]	wt% PyMOI[d]	Repeating unit (n or 2p or 2q)
HO–PEG4600–OH	–	4.9	–	–	–	–	$n = 112$
Br–PEG4600–Br	57.00	5.2	1.03	–	–	–	$n = 111$
PMMA–PEG4600–PMMA	37.68	6.4	1.09	81	19	–	2p = 12
Py–PMMA–PEG4600–PMMA–Py-1	46.42	42.4	1.38	12.2	2.9	84.9	2q = 93
Py–PMMA–PEG4600–PMMA–Py-2	43.68	33.9	1.21	15.3	3.6	81.1	2q = 71
Py–PMMA–PEG4600–PMMA–Py-3	39.78	24.7	1.14	21.0	4.9	74.1	2q = 47
Py–PMMA–PEG4600–PMMA–Py-4	32.79	15.7	1.10	33.0	7.7	59.3	2q = 24

[a] Yield was determined gravimetrically.
[b] Determined by ^{1}H NMR analysis.
[c] Determined by gel permeation chromatography (GPC).
[d] Weight fraction of PEG, PMMA and **PyMOI** in the block copolymer determined by ^{1}H NMR spectroscopy, respectively.

Table 2
Thermal properties of the CBABC-type pentablock copolymers and their precursors.

Sample code	T_g[a] (°C)	T_m[a] (°C)	ΔH_m[a] (J g^{-1})	X_c[b] (%)	X_c[c] (%)	Td_{10}[d] (°C)		Td_1[d] (°C)	Td_2[d] (°C)	Td_3[d] (°C)
						In nitrogen	In air			
HO–PEG4600–OH	–[e]	58.0	160.5	79.1	91.7	382	234	403	–	–
Br–PEG4600–Br	–	53.2	118.2	58.2	62.8	328	235	388	–	–
PMMA–PEG4600–PMMA	–	48.7	106.8	52.6	56.7	323	313	382	–	–
Py–PMMA–PEG4600–PMMA–Py-1	18.2	–	–	–	A	266	266	286	347	396
Py–PMMA–PEG4600–PMMA–Py-2	19.8	–	–	–	A	265	264	286	347	397
Py–PMMA–PEG4600–PMMA–Py-3	21.8	–	–	–	A	277	275	287	353	405
Py–PMMA–PEG4600–PMMA–Py-4	24.7	–	–	–	A	274	275	292	351	395

[a] T_g, T_m and ΔH_m were determined by DSC at a heating rate of 10 °C min^{-1}.
[b] The crystallinity of the sample, X_c, is determined by the equation: $X_c = (\Delta H_m/\Delta H_m^0) \times 100$, where ΔH_m is the melting enthalpy of the sample from the second DSC heating scans and ΔH_m^0 is the melting enthalpy of 100% crystalline PEG ($\Delta H_m^0 = 203$ J g^{-1}). [Reference: Wuderlich, B., Macromolecular Physics, vol. 3, Academic Press, New York, N.Y., 1980.].
[c] The crystallinity of the sample, X_c, is determined from wide-angle X-ray scattering (WAXS). "A" means amorphous.
[d] Td_{10} is the onset decomposition temperature, evaluated as 10% weight loss and was determined by TG at a heating rate of 10 °C min^{-1}; Td_1, Td_2 and Td_3 are the temperatures at the inflection point of the first, second and third decomposition steps in nitrogen.
[e] Not detected.

and the molar ratio of **PyMOI**/**PMMA–PEG4600–PMMA**/CuBr/bipy was 50:1:1:2. Because **PMMA–PEG4600–PMMA** was easily soluble in methanol, the resulting colorless polymer, **Py–PMMA–PEG4600–PMMA–Py**, was precipitated from methanol, then dissolved in CH_2Cl_2 and reprecipitated from methanol multiple times in order to remove impurity such as **PMMA–PEG4600–PMMA**. The structure of the pentablock copolymers was confirmed by FT-IR and NMR spectra. The FT-IR spectrum of **Py–PMMA–PEG4600–PMMA–Py** exhibited absorptions at 3402 (N–H), 1721 (C═O) and 1134 cm^{-1} (C–O–C), confirmed the presence of **PyMOI** segment in the structure. The ^{1}H NMR spectrum of pentablock copolymer is presented in Fig. 1(c). The new signals at 7.2–8.2 and 5.2–5.9 ppm appear for the pentablock copolymer in $CDCl_3$ after ATRP of **PyMOI**. The new resonance signal at 7.2–8.2 ppm was ascribed to the protons of pyrene group and signal between 5.2 and 5.9 ppm was resulted from secondary amine and methylene in the ^{1}H NMR spectrum [Fig. 1(c)]. This observation confirmed the blocking of **PMMA–PEG4600–PMMA** with **PyMOI**. From the weight fraction of **PyMOI** in pentablock copolymers (f_{PyMOI}) (Calculation detail was described in the Supplementary materials, Eq. S2) and $\overline{M}_n$ estimated by ^{1}H NMR of **PMMA–PEG4600–PMMA**, the absolute molecular weight of the corresponding **Py–PMMA–PEG4600–PMMA–Py** was calculated to be 2.47×10^4 g/mol with 47 repeat units of **PyMOI** segment (2q = 47, Scheme 2) in the pentablock copolymer.

Table 1 presents the molecular weight, compositions (PEG, PMMA and **PyMOI** contents in weight) and the number of repeating unit of all pentablock copolymers and their precursors synthesized in this manuscript. The **PyMOI** block length of pentablock copolymer ranges from a few thousand to more than 3×10^4 g/mol, corresponding to 59.3–84.9 wt% in the copolymers. The $\overline{M}_n$ values obtained by GPC of pentablock copolymer were not reliable and lower than the values obtained by ^{1}H NMR. For example, the $\overline{M}_n$ of **Py–PMMA–PEG4600–PMMA–Py-3** given by GPC is 11,600 g/mol, while the theoretical molecular weight is 25,600 g/mol. Xu et al. [17] and Sha et al. [18] also obtained the similar results. The GPC traces of pentablock copolymers and their precursors are shown in Fig. 2 and all of them are with unimodal peaks.

It can be seen that the GPC trace of the block copolymer shifts to the higher molecular weight as increasing **PyMOI** content of pentablock copolymers. Therefore, monomer **PyMOI** is proven to be initiated by macroinitiator **PMMA–PEG4600–PMMA** successfully. The polydispersity index of the copolymers which was listed in Table 1 is a little higher than that of the macroinitiator. However, it is still lower than the theoretical value of 1.5. That means polymer chain end is still carrying out in controlled/"living" free radical polymerization [24].

3.3. Thermal property

The thermal properties of the pentablock copolymers were evaluated by differential scanning calorimeter (DSC) and thermogravimetric analyzer (TGA) and the results are presented in

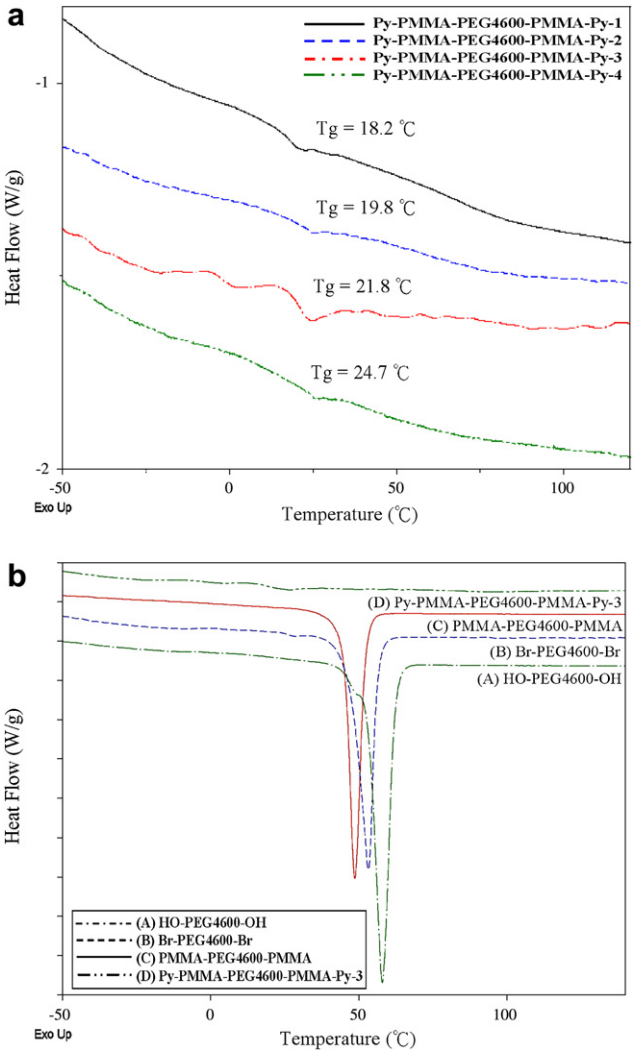

Fig. 3. DSC thermograms of (a) pentablock copolymers (b) **Py–PMMA–PEG4600–PMMA–Py-3** and their precursors at 10 °C/min under steady flow of nitrogen.

Table 2. The DSC thermograms of the pentablock copolymers and their precursors are shown in Fig. 3(a) and (b).

Glass transition temperatures (T_gs) of pentablock copolymers were found to be in the range of 18.2–24.7 °C in Fig. 3(a). The result shows the T_g of pentablock copolymers increases as **PyMOI** segment decreases. It is probable that introducing of flexible bridge linkage (ether unit and aliphatic group) of **PyMOI** into the polymer backbone tends to increase the free rotation of the polymer molecule. In Fig. 3(b), it indicated that the melting temperature (T_m) and the melting enthalpy (ΔH_m) of triblock copolymer were decreased slightly with incorporating PMMA segment, which indicated that their non-isothermal crystallization rate decreased with existing PMMA segments. The melting temperature of the pentablock copolymers was not observed in DSC thermograms. It is because that incorporation of the bulky pyrene substituent into pentablock copolymers disturbs the regular packing of triblock copolymer. The crystalline PEG shows two distinct and sharp Bragg reflections at 2θ values of 18.8° (the 120 reflection) and 23.1° (combination of the PEO 112 and 032 reflections) [40,48], and the crystallinity ($X_c = 56.7$–91.7%, Table 2) of pentablock copolymers and their precursors obtained from wide-angle X-ray scattering (WAXS) was consistent with the results of DSC. The X-ray diffractograms of pentablock copolymers and their precursors were shown in Fig. 4.

The temperatures at 10% weight loss (Td_{10}), examined by TG analysis, showed values ranging from 265 to 323 °C in nitrogen and 264 to 313 °C in air. It was observed that the Td_{10} will decrease while incorporating the **PyMOI** into the triblock copolymer. It is probable that introducing of flexible bridge linkage (ether unit and aliphatic group) of **PyMOI** into the polymer backbone tends to decrease the Td_{10} values. All of the block copolymers showed higher Td_{10} in nitrogen than in air. In general, thermal degradation under nitrogen of standard radically prepared PMMA proceeds in three steps corresponding respectively to the head-to-head linkage (around 165 °C), the chain-end initiation from the vinylidene ends (around 270 °C), and the step referred to as random scission within the polymer chain (around 360 °C) [49]. Thermal degradation of the triblock copolymer occurred around 382 °C corresponding to combination of the PEO segments and random scission within PMMA chain. This result is a further indication of the absence of abnormal linkages in triblock copolymer, such as the head-to-head linkages and vinylidene ends, therefore confirming the high regioselectivity and the virtual absence of termination reactions. In Fig. 5 thermal degradation of pentablock copolymers showed a three-step degradation, with steps corresponding respectively to the **PyMOI** segments [around 286 °C (Td_1)], random scission within the PMMA chain [around 350 °C (Td_2)], and the step referred to as PEO segment [around 400 °C (Td_3)] [50,51]. It is clearly obvious that the decomposition temperature of **PyMOI** segment was around 286 °C (Td_1) in pentablock copolymer. The TGA spectrum of **PyMOI** is shown in the Supplementary materials, Fig. S1. It was clearly to observe that 10 wt% loss degradation temperature of **PyMOI** was at 293 °C. This result can support the decomposition temperature of **PyMOI** segment was around 286 °C (Td_1) in pentablock copolymer and was also evidenced that the monomer **PyMOI** was incorporated into triblock copolymer successfully.

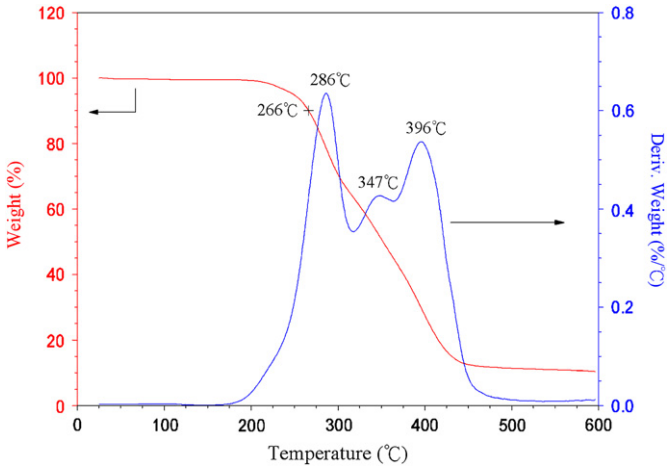

Fig. 5. TGA curve of **Py–PMMA–PEG4600–PMMA–Py-1** obtained by heating from room temperature to 600 °C at 10 °C/min under steady flow of nitrogen.

3.4. Optical property

The fluorescence emission spectra of the **PyMOI** [Fig. 6(A)] and **Py–PMMA–PEG4600–PMMA–Py** [Fig. 6(B)–(E)] were recorded in

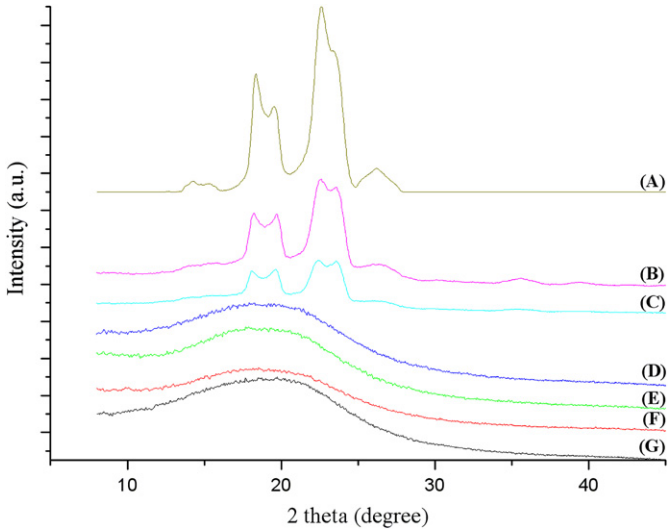

Fig. 4. The wide-angle X-ray diffractograms of (A) **HO–PEG4600–OH**; (B) **Br–PEG4600–Br**; (C) **PMMA–PEG4600–PMMA**; (D) **Py–PMMA–PEG4600–PMMA–Py-1**; (E) **Py–PMMA–PEG4600–PMMA–Py-2**; (F) **Py–PMMA–PEG4600–PMMA–Py-3** and (G) **Py–PMMA–PEG4600–PMMA–Py-4**.

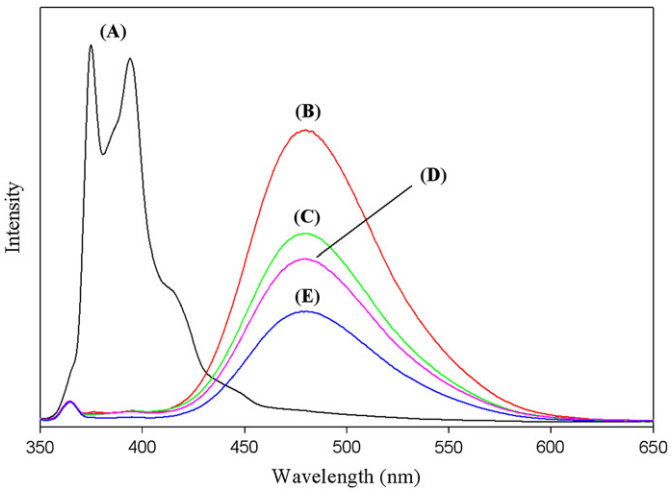

Fig. 6. Fluorescence spectra of (A) **PyMOI**; (B) **Py–PMMA–PEG4600–PMMA–Py-1**; (C) **Py–PMMA–PEG4600–PMMA–Py-2**; (D) **Py–PMMA–PEG4600–PMMA–Py-3** and (E) **Py–PMMA–PEG4600–PMMA–Py-4** in THF; polymer concentration: 1.85×10^{-4} mg/mL; $\lambda_{ex} = 330$ nm, $T = 25$ °C.

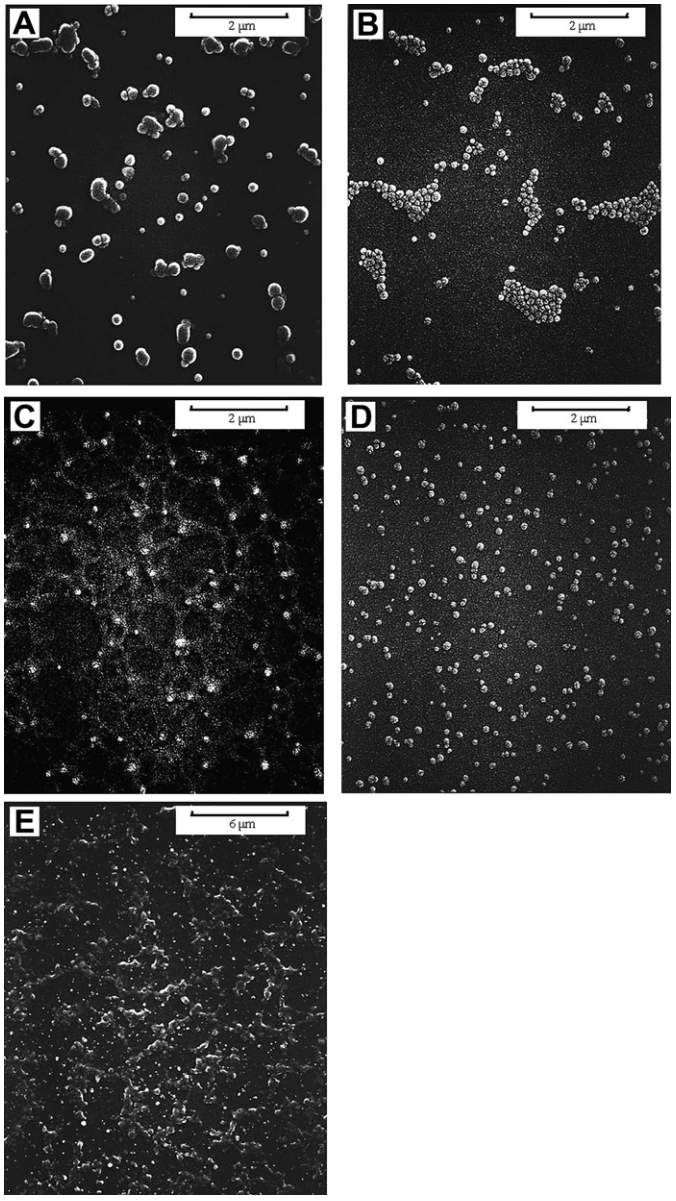

Fig. 7. SEM micrographs of (A) **Py–PMMA–PEG4600–PMMA–Py-1** (0.1 mg/mL); (B) **Py–PMMA–PEG4600–PMMA–Py-2** (0.1 mg/mL); (C) **Py–PMMA–PEG4600–PMMA–Py-3** (0.1 mg/mL); (D) **Py–PMMA–PEG4600–PMMA–Py-4** (0.1 mg/mL); (E) **Py–PMMA–PEG4600–PMMA–Py-1** (1.0 mg/mL).

THF at constant monomer or polymer concentration (1.85×10^{-4} mg/mL) and room temperature by excitation at 330 nm wavelength. Fluorescence spectra of **PyMOI** exhibited strong monomer emission occurring in the near-UV at *ca.* 375 and 394 nm due to locally isolated excited pyrenes (pyrene "monomer" emission) and did not show a board excimer emission at higher wavelengths. Fluorescence spectra of **Py–PMMA–PEG4600–PMMA–Py-1** exhibited stronger excimer emission at *ca.* 480 nm. It was probable due to the chromophores linked to distant units along the polymer backbone are brought into close proximity within aggregates formed *via* interaction of the hydrophobic chains [35,36,42,52,53]. In Fig. 6(B)–(E) it is clearly obvious that there were the higher emission intensity at *ca.* 480 nm when increasing composition of **PyMOI** in pentablock copolymers (1.85×10^{-4} mg/mL). It is probable that the intensity of emission will increase when increasing the chain length of **PyMOI** in pentablock copolymers.

3.5. Morphology in SEM micrograph

It is interesting to find the individual aggregates of pentablock copolymers (**Py–PMMA–PEG4600–PMMA–Py-1 to Py–PMMA–PEG4600–PMMA–Py-4**) in SEM micrographs, as shown in Fig. 7.

The average diameters of pentablock copolymers [**Py–PMMA–PEG4600–PMMA–Py-1** [Fig. 7(A)], **Py–PMMA–PEG4600–PMMA–Py-2** [Fig. 7(B)], **Py–PMMA–PEG4600–PMMA–Py-3** [Fig. 7(C)] and **Py–PMMA–PEG4600–PMMA–Py-4** [Fig. 7(D)]] in SEM micrographs were calculated as *ca.* 210, 158, 131 and 110 nm, respectively. It is clearly obvious that there were larger aggregates when increasing composition of **PyMOI** in pentablock copolymers. It may be due to intra-aggregate interactions occurred mainly in pentablock copolymers as described in the published paper [41]. The same trend has been observed in TEM micrographs of PLG-*b*-PEG block copolymers [54]. In addition, clear morphology changes are observed as a function of the concentration of the polymer solution [Fig. 7(A) and (E)]. The spherical [Fig. 7(A), 0.1 mg/mL] morphology changed into chainlike aggregate [Fig. 7(E), 1.0 mg/mL] because of the different concentration of pentablock copolymers in THF. It may be due to the inter-aggregate interactions occurred mainly in pentablock copolymers [55–60].

4. Conclusions

New amphiphilic fluorescent CBABC-type pentablock copolymers containing pyrene group reinitiated by **PMMA–PEG4600–PMMA** macroinitiator were successfully synthesized by ATRP in two steps. All of the pentablock copolymers synthesized in this work have relatively narrow molecular weight distributions, unimodal peaks in GPC traces and good compatibility. The crystallinity of PEG segment was destroyed by incorporating PMMA and **PyMOI** segments. Fluorescence spectra of **Py–PMMA–PEG4600–PMMA–Py** exhibited stronger excimer emission at *ca.* 480 nm. Increasing the composition of **PyMOI** in amphiphilic pentablock copolymers obtained larger aggregate size. Furthermore, the morphology became chainlike aggregates as the concentration of pentablock copolymers up to 1.0 mg/mL.

Acknowledgments

The authors would like to thank the National Science Council of the Republic of China for the financial support of this work. The authors thank Prof. Kajiwara, A. (Nara University of Education, Japan) for his valuable comments.

Appendix. Supplementary data

Supplementary data associated with this article can be found in the online version, at doi:10.1016/j.polymer.2009.08.042.

References

[1] Hadjichristidis H, Pispas S, Floudas G. Block copolymers: synthetic strategies, physical properties, and applications. Hoboken, NJ: Wiley-Interscience; 2003.
[2] Webster OW. Science 1991;251:887–93.
[3] Matyjaszewski K, Xia JH. Chem Rev 2001;101:2921–90.
[4] Kamigaito M, Ando T, Sawamoto M. Chem Rev 2001;101:3689–745.
[5] Wang JS, Matyjaszewski K. J Am Chem Soc 1995;117:5614–5.
[6] Kato M, Kamigaito M, Sawamoto M, Higashimura T. Macromolecules 1995;28:1721–3.
[7] Kagawa Y, Minami H, Okubo M, Zhou J. Polymer 2005;46:1045–9.
[8] Lowe AB, Sumerlin BS, McCormick CL. Polymer 2003;44:6761–5.
[9] Laruelle G, Parvole J, Francois J, Billon L. Polymer 2004;45:5013–20.
[10] Zhang H, Yu Z, Wan X, Zhou QF, Woo EM. Polymer 2002;43:2357–61.
[11] Theis A, Feldermann A, Charton N, Davis TP, Stenzel MH, Barner-Kowollik C. Polymer 2005;46:6797–809.
[12] Qin DQ, Qin SH, Chen XP, Qiu KY. Polymer 2000;41:7347–53.

[13] Carlmark A, Vestberg R, Jonsson EM. Polymer 2002;43:4237–42.
[14] Matyjaszewski K, Patten TE, Xia JH. J Am Chem Soc 1997;119:674–80.
[15] Hua D, Bai R, Lu W, Pan CY. J Polym Sci Part A Polym Chem 2004;42:5670–6.
[16] Ravi P, Sin SL, Gan LH, Gan YY, Tam KC, Xia XL, et al. Polymer 2005;46:137–46.
[17] Xu K, Wang Y, Bai R, Lu WQ, Pan CY. Polymer 2005;46:7572–7.
[18] Sha K, Li D, Li Y, Zhang B, Wang J. Macromolecules 2008;41:361–71.
[19] Ling J, Chen W, Shen Z. J Polym Sci Part A Polym Chem 2005;43:1787–96.
[20] Thunemann AF, Kubowicz S, von Berlepsch H, Mohwald H. Langmuir 2006;22:2506–10.
[21] Toman L, Janata M, Sikora A. J Polym Sci Part A Polym Chem 2004;42: 6098–108.
[22] Tu RS, Tirrell M. Adv Drug Delivery Rev 2004;56:1537–63.
[23] Lutz JF, Laschewsky A. Macromol Chem Phys 2005;206:813–7.
[24] Liaw DJ, Chen TP, Huang CC. Macromolecules 2005;38:3533–8.
[25] Davis KA, Matyjaszewski K. Macromolecules 2001;34:2101–7.
[26] Nicolaÿ R, Kwak Y, Matyjaszewski K. Macromolecules 2008;41:4585–96.
[27] Tsarevsky NV, Sarbu T, Göbelt B, Matyjaszewski K. Macromolecules 2002;35:6142–8.
[28] Kopchick JG, Storey RF, Beyer FL, Mauritz KA. Polymer 2007;48:3739–48.
[29] Liu C, Wang G, Zhang Y, Huang J. J Appl Polym Sci 2008;108:777–84.
[30] Ramakrishnan A, Dhamodharan R. Macromolecules 2003;36:1039–46.
[31] Darcos V, Haddleton DM. Eur Polym J 2003;39:855–62.
[32] Zhang H, Sun X, Wang X, Zhou QF. Macromol Rapid Commun 2005;26:407–11.
[33] Toman L, Janata M, Spěváček J, Vlček P, Látalová P, Sikora A, et al. J Polym Sci Part A Polym Chem 2005;43:3823–30.
[34] Eastwood EA, Dadmun MD. Macromolecules 2001;34:740–7.
[35] Sun X, Zhang H, Huang X, Wang X, Zhou QF. Polymer 2005;46:5251–7.
[36] Winnik FM. Chem Rev 1993;93:587–614.
[37] Enomoto Y, Kamitakahara H, Takano T, Nakatsubo F. Cellulose 2006;13:437–48.
[38] Repáková J, Holopainen JM, Karttunen M, Vattulainen I. J Phys Chem B 2006;110:15403–10.
[39] Liaw DJ, Huang CC, Sang HC, Kang ET. Langmuir 1998;14:3195–201.
[40] Liaw DJ, Huang CC, Sang HC, Kang ET. Langmuir 1999;15:5204–11.
[41] Liaw DJ, Wang KL, Chen TP, Lee KR, Lai JY. Polymer 2007;48:3694–702.
[42] Lutz JF, Hoth A. Macromolecules 2006;39:893–6.
[43] Nakahara Y, Kida T, Nakatsuji Y, Akashi M. J Org Chem 2004;69:4403–11.
[44] Kajiwara A, Matyjaszewski K, Kamachi M. Macromolecules 1998;31:5695–701.
[45] Jankova K, Chen X, Kops J, Batsberg W. Macromolecules 1998;31:538–41.
[46] He X, Zhang H, Yan D, Wang X. J Polym Sci Part A Polym Chem 2003;41: 2854–64.
[47] Bailey FE, Koleske JV. Poly(ethylene oxide). New York: Academic Press; 1976.
[48] Bortel E, Hodorowicz S, Lamot R. Makromol Chem 1979;180:2491–8.
[49] Granel C, Dubois PH, Jérôme R, Teyssié PH. Macromolecules 1996;29:8576–82.
[50] Signori F, Chiellini F, Solaro R. Polymer 2005;46:9642–52.
[51] Bahadur KCR, Bhattarai SR, Aryal S, Khil MS, Dharmaraj N, Kim HY. Colloids and Surfaces A Physicochem Eng Aspects 2007;292:69–78.
[52] Morishima Y. Adv Polym Sci 1992;104:51–96.
[53] Birks JB. Rep Prog Phys 1975;38:903–74.
[54] Riley T, Stolnik S, Heald CR, Xiong CD, Garnett MC, Illum L, et al. Langmuir 2001;17:3168–74.
[55] Yu K, Eisenberg A. Macromolecules 1996;29:6359–61.
[56] Zhang L, Eisenberg A. Science 1995;268:1728–31.
[57] Zhang L, Eisenberg A. J Am Chem Soc 1996;118:3168–81.
[58] Zhang L, Eisenberg A. Macromolecules 1999;32:2239–49.
[59] Yu K, Eisenberg A. Macromolecules 1998;31:3509–18.
[60] Cheyne RB, Moffitt MG. Langmuir 2006;22:8387–96.